

*Original Scientific Article***COMPUTER TOMOGRAPHY (CT) SCANS AS A DIAGNOSTIC TOOL FOR INTERPRETATION OF S10 PLASTINATED SLIDES FROM DOG CADAVER**

Lazo Pendovski¹, Dimitar Bozhinovski¹, Ksenija Ilievska²,
Plamen Trojachanec², Vlatko Ilieski¹

¹*Department of Functional Morphology, Faculty of Veterinary Medicine-Skopje, Ss. Cyril and Methodius University, Lazar Pop-Trajkov 5-7, 1000 Skopje, North Macedonia*

²*Department of Veterinary Surgery, Faculty of Veterinary Medicine-Skopje, Ss. Cyril and Methodius University, Lazar Pop-Trajkov 5-7, 1000 Skopje, North Macedonia*

Received 9 February 2022; Received in revised form 8 April 2022; Accepted 11 April 2022

ABSTRACT

Computed tomography (CT) is a routine method for the diagnosis of pathological structures in the body and has been widely used in veterinary medicine as an advanced diagnostic imaging tool in veterinary clinics. However, interpretation of CT scans requires detailed knowledge of topographical animal anatomy and usually has limited scan resolution due to the ambiguous relationship between signal intensity and tissue composition. The aim of the study was to assess the morphometric similarities between S10 plastinated slides and computer tomography (CT) scans and their usability as compatible paired diagnostic methods. A 3-year-old euthanized dog cadaver was scanned on SHIMADZU SCT/6800TXL scanner immediately post-mortem, then frozen at -80 °C to preserve the correct anatomical position, and plastinated with a standardized procedure. Semi-transparent transversal slices (5 mm) were obtained from the head, thoracic, and lumbar sections of the body. The S10 plastinated slides and CT scans contained fine and small anatomical structures with high similarity. The spatial relationships of all anatomical structures on the serial S10 plastinates were in the correct anatomical position. In conclusion, S10 transversal slices showed high similarity with the CT scans and allowed identification of the corresponding morphological structures. The S10 thin plastinated transversal slices could be used for additional interpretation of CT transversal scans at veterinary clinics and as a didactical tool for veterinary students.

Key words: S10 plastination, computer tomography (CT), topographic anatomy, dog

INTRODUCTION

Computed tomography (CT) as a routine method for the diagnosis of diseases in human medicine has been widely used in the last 50 years (1). In the late 90's, CT was introduced in veterinary medicine and appeared to be an advanced diagnostic imaging tool in veterinary clinics, since many of the diseases in pet animals can only be diagnosed with the help of CT or magnet resonance scans (2). However, the

interpretations of CT scans or the differentiation of pathological from normal anatomical structures require detailed knowledge of the topographic anatomy of animals (3). Nowadays, scientists often prefer plastination as one of the most effective tools for easier study of topographic anatomy in animals, especially on thin cross-sectionalized plastinated slices/models, due to the ability to retain the same morphometric characteristics (3, 4). Many studies have compared thin plastinated slices with CT or magnetic resonance imaging (MRI) (4, 5, 6). The process of plastination itself proves to be an indispensable tool in the study of animal anatomy, as well as in facilitating the work in clinics, especially for clinical anatomists (7). In clinical practice, plastination, especially plastinated thin slices, can be used for diagnostic and therapeutic aims in advanced surgery, i.e., surgical anatomy forming a bridge between morphology and clinical practice (8).

Corresponding author: Prof. Lazo Pendovski, PhD

E-mail address: lpendovski@fvm.ukim.edu.mk

Present address: Department of Functional Morphology, Faculty of Veterinary Medicine-Skopje, Ss. Cyril and Methodius University, Lazar Pop-Trajkov 5-7, 1000 Skopje, North Macedonia

Phone: +389 2 3240 728

Copyright: © 2022 Pendovski L. This is an open-access article published under the terms of the Creative Commons Attribution License which permits unrestricted use, distribution, and reproduction in any medium, provided the original author and source are credited.

Competing Interests: The authors have declared that no competing interests exist.

Available Online First: 18 April 2022

Published on: 15 October 2022

<https://doi.org/10.2478/macvetrev-2022-0020>

The study aimed to assess the morphometric similarities between S10 plastinated slides and computer tomography (CT) scans and their usability as compatible paired diagnostic methods.

MATERIAL AND METHODS

In this study, we used a 3-year-old euthanized dog cadaver without pathological or anatomical changes. The dog was fixed in the desired position and was placed in dorsal recumbency for taking CT scans. The cadaver's neck, head, and thoracic limbs were placed in maximal extension in the cranial direction. The hind limbs and the pelvis were positioned in the caudal extension (5, 9). Auxiliary methods were used to properly position the cadaver by using strips or bands around the limbs and body (Fig. 1A).

A CT scanner SCT SHIMADZU 6800TXL was used at the Animal Hospital "Postojna" in Slovenia. The scans of each section were taken in 5 mm thickness, cranial-caudal direction, without (native) or with a high-pitch resolution for

better contrast and differentiation of bones and soft tissues. The images were taken by applying standard protocol (80kV, the effective mA was 100 to 0.5) with a rotation time of 0.6 seconds (2). They were reconstructed by the B31s algorithm. A 1.2 mm detector was used for reconstructing the 5 mm thickness scans (Fig. 2).

After the CT scan was completed, the dog was immediately frozen at -80°C (Fig. 1B) to preserve the correct position needed for obtaining the slices during the plastination. The slicing and plastination were performed according to the method described by Pendovski et al. (10). The frozen cadaver was cut into four body parts using a band saw. Each body part was immediately returned at -80°C (Fig. 1C). Transversal 5 mm slices were cut from the head, thoracic, and lumbar sections of the body (Fig. 1D). The dehydration process (Fig. 1E) was performed with cold acetone (-25°C) in a 10:1 ratio with the slices (11). The step of forced impregnation (Fig. 1F) was performed at -25°C with a mix of silicone (S10 with S3, in a 100:0.5 ratio) (11). The modeling of the slices was performed with S6 silicone in 5% concentration (Fig. 1G) (12).

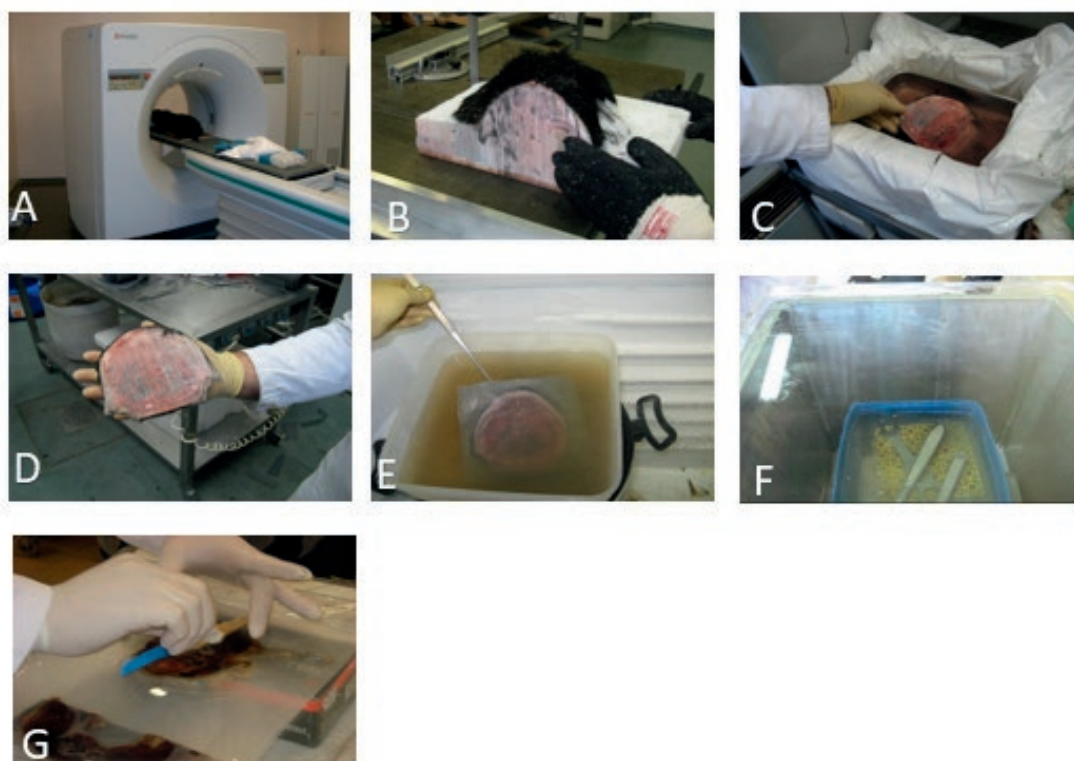


Figure 1. Position of the dog for CT imaging (A); Freezing of the dog-cadaver (B); Cutting the dog-cadaver (C); Preparing slices with 5 mm thickness (D); Dehydration stage of plastination (E); Forced impregnation (F); Curing and modeling stage of plastinated slices (G)

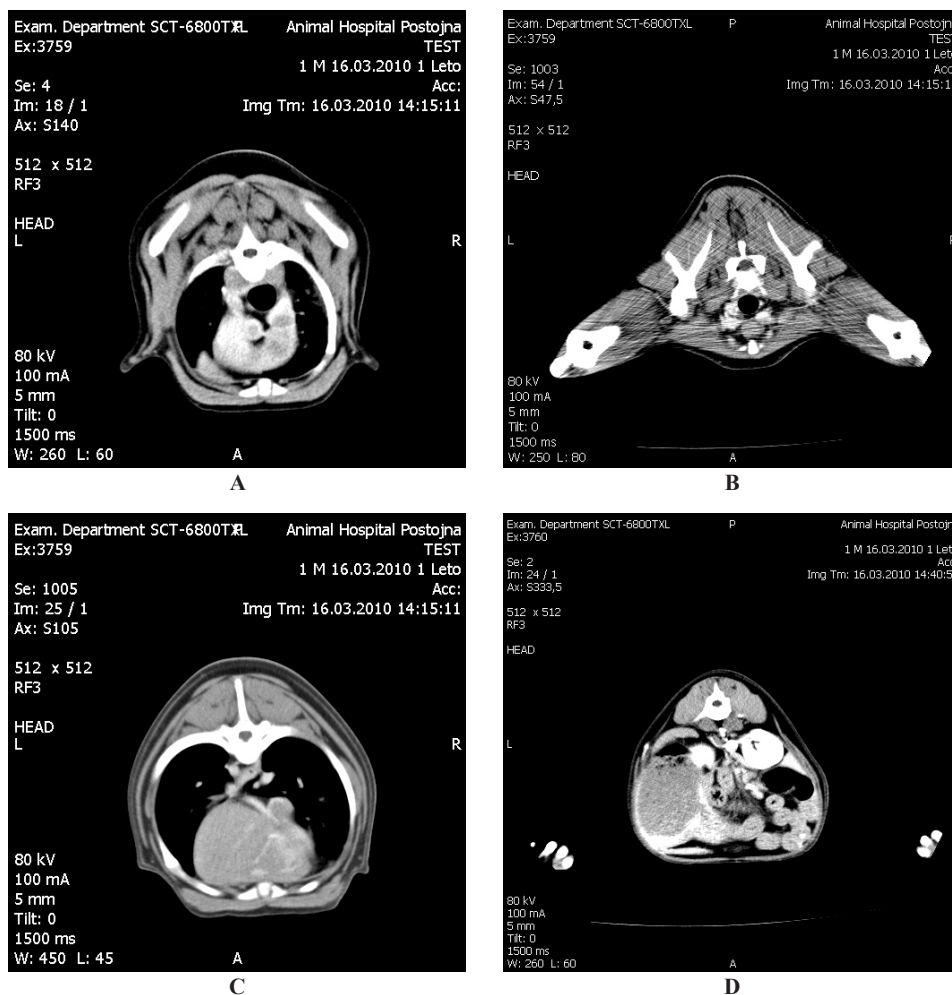


Figure 2. CT scans on different levels: Thorax (A); Pelvis (B); Thorax (C); Abdomen (D)

The plastinated models were photographed (scanned) with the corresponding CT scans' level/angle. Comparisons were made on the following anatomical regions: first molar tooth (M1) (sinuses, muscles, glands, bones, globe of the eye, nasal turbinate), second thoracic vertebra (T2) (muscles, blood vessels, bones, organs: esophagus, heart, pericardium, valves), fourth thoracic vertebra (T4) (muscles, blood vessels, bones, organs: esophagus, heart, pericardium, valves), first lumbar vertebra (L1) (muscles, blood vessels, bones, organs: esophagus, heart, pericardium, valves), and fourth lumbar vertebra (L4) (muscles, blood vessels, organs: small and large intestines, kidneys, lymph nodes, lien).

RESULTS

The photographs of plastinated slices and CT scans are presented in Figures 3-7.

The compared anatomical structures (glands, blood vessels, pyloric thickness, major nerves) were highly comparable between the plastinated transverse sections and CT scans. The corresponding structures were equally visible and identifiable in the plastinated slices, CT scan, and native photography.

In M1 region (Fig. 3) the following anatomical structures were easily recognizable and highly comparable between the three scanned models: bones (zygomatic arc, mandible, maxilla, molar tooth I), muscles (pterygoid, genioglossus, and ventral oblique muscle), cavities (frontal sinus, ethmoidal conchae, oral cavity), zygomatic gland, hard palate, bulbus olfactorius, ocular globe (bulbus oculi). The pterygoid muscle and the zygomatic gland are specific anatomical structures that were highly identifiable (red circles in Fig. 3).

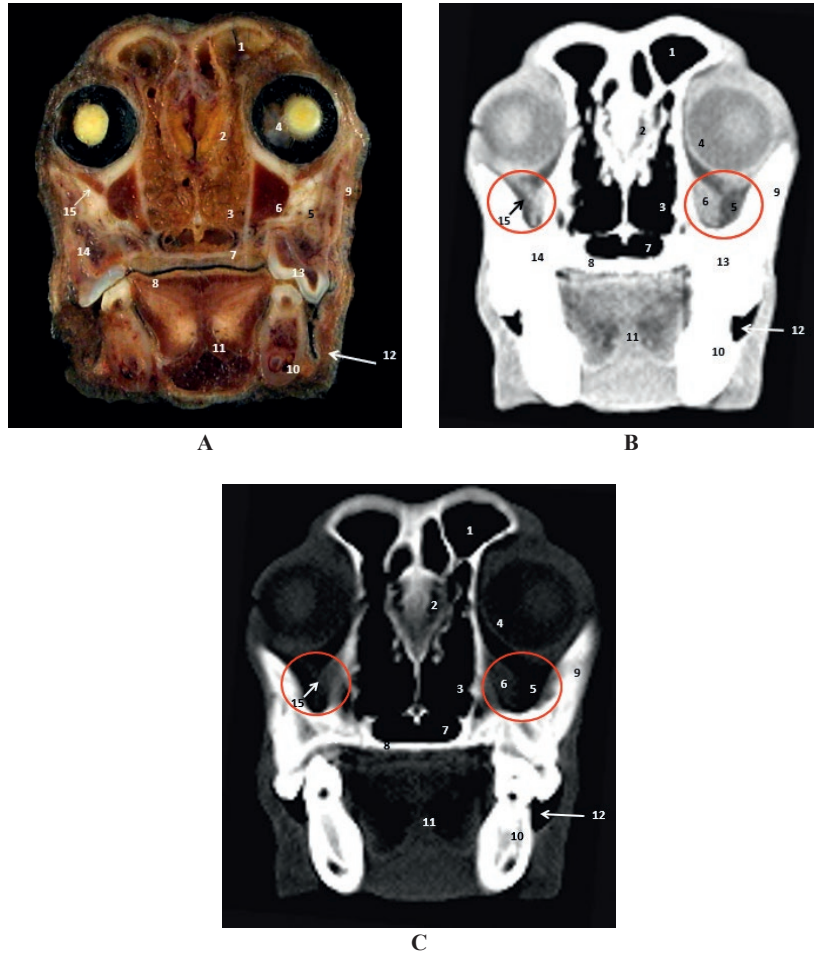


Figure 3. A. Plastinated slice on level of first molar tooth (M1); B. CT scan (high-pitch); C. CT scan (native): 1. frontal sinus; 2. bulbus olfactorius; 3. ethmoidal conchae; 4. bulbus oculi; 5. zygomatic gland; 6. pterygoid muscle; 7. choana; 8. hard palate; 9. zygomatic arch; 10. mandible; 11. genioglossus muscle; 12. oral cavity; 13. moral tooth I; 14. maxilla; 15. ventral oblique muscle

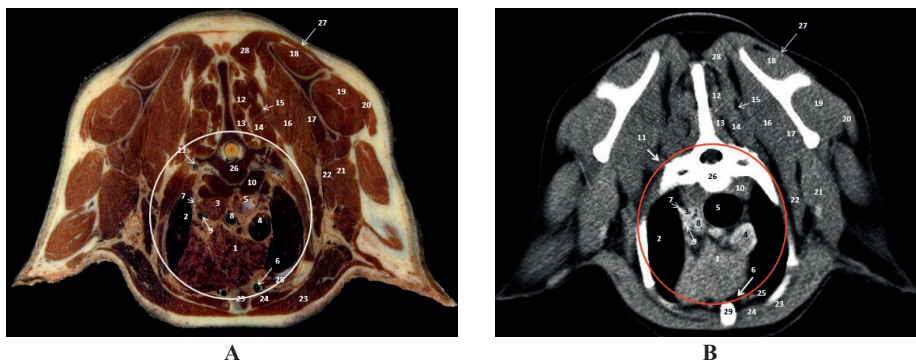


Figure 4. A. Plastinated slice level of second thoracic vertebra (T2); B. CT scan (native): 1. thymus; 2. left cranial pulmonic lobe; 3. esophagus; 4. cranial vena cava; 5. trachea; 6. internal thoracic artery and vein; 7. left subclavian artery; 8. brachiocephalic trunk; 9. left common carotid artery; 10. longus colli muscle; 11. vertebral artery; 12. spinalis thoracis muscle; 13. multifidus thoracis muscle; 14. semispinalis capitis muscle; 15. splenius muscle; 16, 17. ventral serratus muscle; 18. supraspinatus muscle; 19. infraspinatus muscle; 20. deltoideus muscle; 21. triceps brachii muscle; 22. teres major muscle; 23. pectoral muscle; 24. rectus thoracis muscle; 25. transversus thoracis muscle; 26. thoracic vertebra II; 27. trapezius muscle; 28. rhomboideus muscle; 29. sternum

In the T2 region (Fig. 4) a large group of chest and back muscles was easily visible (longus colli, spinalis thoracis, multifidus, semispinalis, splenius, ventral serratus, and supraspinatus muscle). In the middle part of Fig. 4 (A-white and B-red circle) the following anatomic structures were easily recognizable and highly comparable between the three scanned models: organs (lungs, esophagus, trachea), glands (thymus), and blood vessels (cranial vena cava, internal thoracic vein, left subclavian artery, brachiocephalic trunk, and left common carotid artery).

In the T4 region, back and chest muscles (trapezius, longissimus, multifidus, latissimus dorsi, iliocostalis, ventral serratus, and deep pectoral muscle) were easily recognizable and comparable (Fig. 5). In the red circle mark (Fig. 5A, B, C) the following structures were easily recognizable and highly comparable between the three scanned models: organs (heart and parts of left and right atria and ventricles, pericardium, bicuspid valves, lung lobes, and esophagus), blood vessels (left pulmonic artery, aorta, right azygous vein, thoracic vein, and artery).

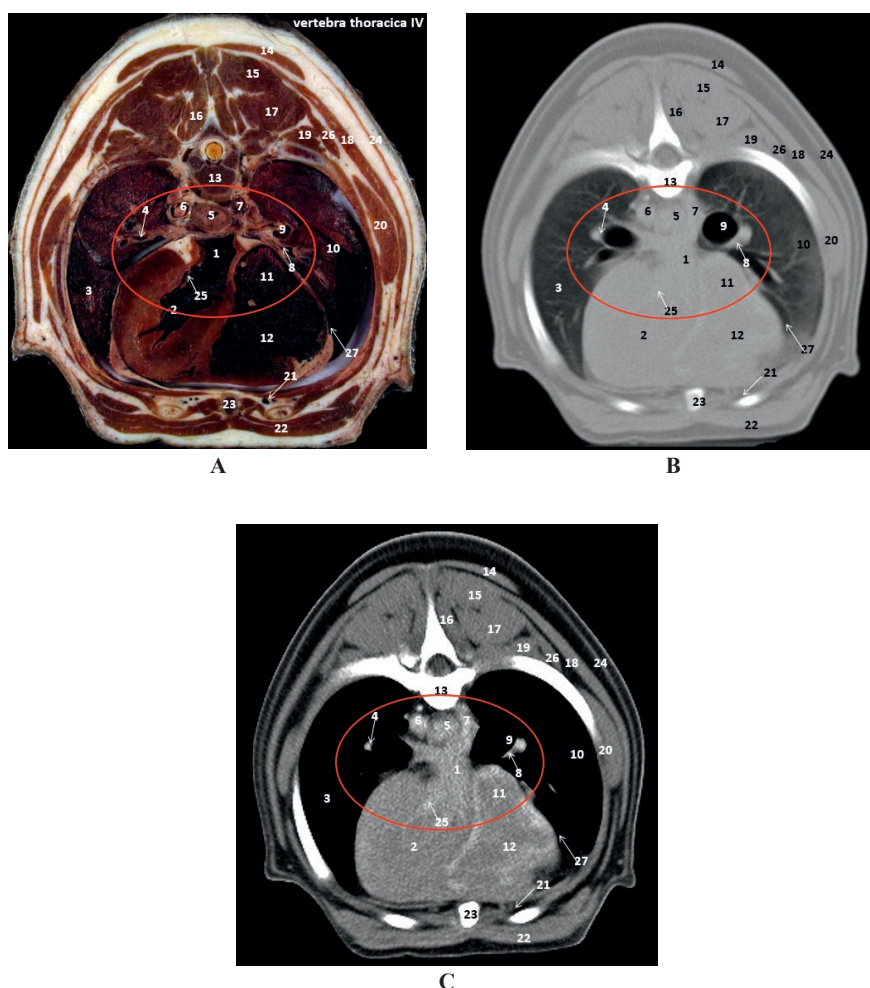


Figure 5. A. Plastinated slice level of fourth thoracic vertebra (T4); B. CT scan (high-pitch); C. CT scan (native): 1. left atrial chord; 2. left ventricular chord; 3. left lung; 4. left pulmonic artery; 5. esophagus; 6. aorta; 7. right azygous vein; 8. right pulmonic artery; 9. bronchus; 10. right lung; 11. right atrial chord; 12. right ventricle; 13. fourth thoracic vertebra; 14. trapezius muscle; 15. semispinalis thoracis muscle; 16. multifidus; 17. longissimus dorsi muscle; 18. latissimus dorsi muscle; 19. iliocostalis muscle; 20. ventral serratus thoracis muscle; 21. internal thoracic artery and vein; 22. deep pectoral muscle; 23. sternum; 24. cutaneous trunci muscle; 25. bicuspid valves; 26. cranial dorsal serrate muscle; 27. pericardium

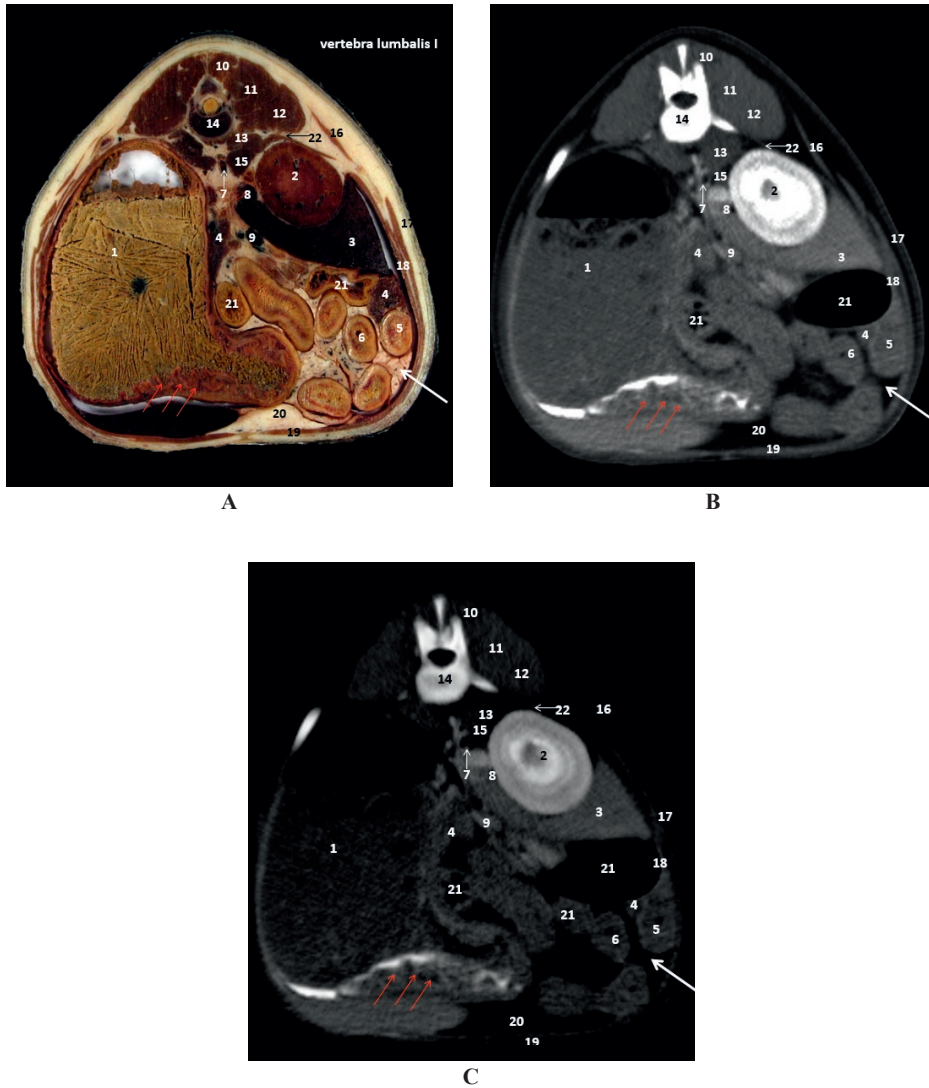


Figure 6. A. Plastinated slice level of first lumbar vertebra (L1); B. CT scan (high-pitch); C. CT scan (native): 1. stomach (red arrows-pyloric thickness); 2. right kidney; 3. liver (caudate process); 4. pancreas; 5. duodenum; 6. jejunum; 7. aorta; 8. caudal cava vein; 9. portal vein; 10. multifidus muscle; 11. longissimus muscle; 12. iliocostalis muscle; 13. quadratus lumborum muscle; 14. first lumbar vertebra; 15. psoas muscle; 16. dorsal serratus caudalis muscle; 17. external abdominal oblique muscle; 18. transverse abdominal muscle; 19. rectus abdominis muscle; 20. falciform ligament; 21. colon; 22. diaphragm. Red arrows: stomach with ingested gastric content

In the L1 region (Fig. 6A, B, C), the back muscles (multifidus, longissimus, iliocostalis, and quadratus lumborum muscle), organs (stomach with ingested content and pylorus, kidney, small intestine, liver), and blood vessels (aorta, caudal vena cava, and portal vein) were easily recognizable and highly comparable between the three scanned models.

In Fig. 7, the back muscles (quadratus lumborum muscle, multifidus, iliocostalis, longissimus, and

psoas major and minor), stomach muscles (external and internal abdominal oblique, rectus abdominis, and transverse abdominal muscle), organs (kidney, small and large intestine, spleen, and pancreas) lymph nodes, and blood vessels (caudal vena cava, renal artery, and aorta) were easily recognizable and highly comparable between the three scanned models.

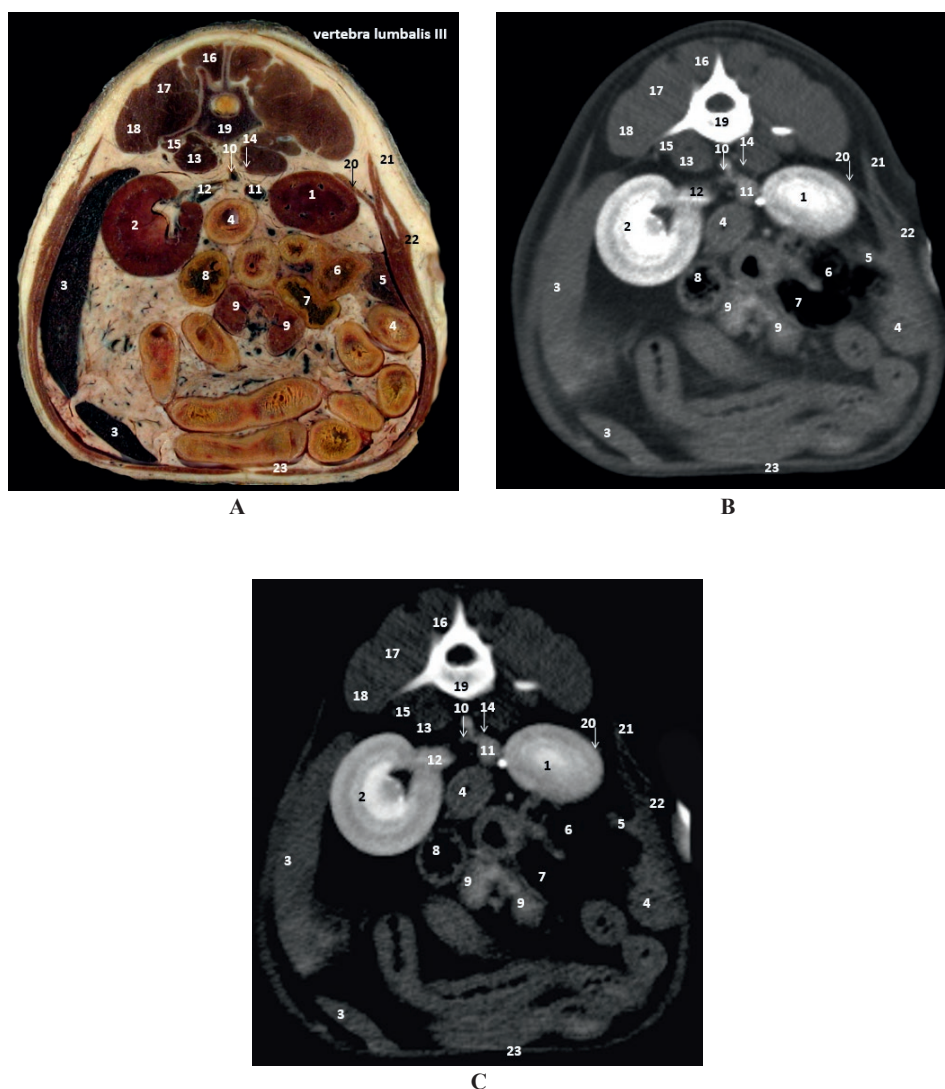


Figure 7. A. Plastinated slice fourth lumbar vertebra (L4); B. CT scan (high-pitch); C. CT scan (native): 1. right kidney; 2. left kidney; 3. spleen; 4. duodenum; 5. pancreas; 6. cecum; 7. colon; 8. jejunum; 9. jejunal lymph nodes; 10. abdominal aorta; 11. caudal vena cava; 12. renal artery and vein; 13. psoas major muscle; 14. psoas minor; 15. quadratus lumborum muscle; 16. multifidus muscle; 17. longissimus muscle; 18. iliocostalis muscle; 19. third lumbar vertebra; 20. transverse abdominis muscle; 21. internal oblique abdominis muscle; 22. external oblique abdominis muscle; 23. rectus abdominis muscle

DISCUSSION

CT is an important diagnostic tool in veterinary medicine able to scan and visualize large and fine anatomical structures in the body yielding easier, faster, and more accurate diagnosis (13). CT is used as an important tool in research and scientific activity contributing to more advanced study designs (14). CT images usually visualize the body in transverse planes of different thickness. It is also

possible to transverse CT images and rearrange them into sagittal or frontal planes using certain software programs contributing to a more accurate and concise diagnosis (15).

Numerous studies reported that thin plastinated models are a useful tool for pre-training programs for CT and MRI (3, 6, 16). The plastinated models retain the fine structure and topography of the corresponding native slices with a translucent layer of connective and lipid tissues, rendering arteries

and veins easily visible (17). An important part that makes our study different from the previous studies is that we used thin plastinated models instead of using frozen cadavers (3, 18).

In this study, the CT scans proved to be a useful tool for comparison of thin plastination models of a dog's body. Each plastinated slice and correspondent CT scan provided detailed information on the topographic anatomy of the dog cadaver. Our findings are similar with other investigators that preformed similar research (3, 5, 6, 16, 17). No topographic changes were found in the thin plastinated models compared to the corresponding CT scans. The plastinated models are long-lasting and could replace frozen cadavers which are routinely used for teaching and demonstrating purposes (3, 18).

CONCLUSION

The S10 plastinated transversal sliced models of dog cadaver successfully reproduced the anatomical and topographic features of the corresponding CT scanned sections. The plastinated models could therefore be used as a didactical and diagnostic tool for veterinary students, practitioners, and researchers.

CONFLICT OF INTEREST

The authors declare that they have no potential conflict of interest with respect to the authorship and/or publication of this article.

ACKNOWLEDGMENTS

The study was conveyed as part of the scientific research project „The Western Balkans University Network for Animal Welfare” (WBVN/RSPCA/2008/01) with RSPCA International. This research was supported by the Faculty of Veterinary Medicine – Skopje.

AUTHORS' CONTRIBUTION

LP conceived and designed the study, supervised the experiments and data analysis, interpreted the results, performed a major part of the experiments and wrote the manuscript. DB interpreted the results and wrote the manuscript. KI, PT participated in computed

tomography interpretations and monitored manuscript writing. VI supervised the study and manuscript writing. All authors have revised and approved the final version of the manuscript.

REFERENCES

1. Brenner, D.J., Hall, E.J. (2007). Computed tomography - an increasing source of radiation exposure. *NEJM* 357(22): 2277-2284. <https://doi.org/10.1056/NEJMra072149> PMid:18046031
2. Randall, E.K. (2016). PET-computed tomography in veterinary medicine. *Vet Clin North Am Small Anim.* 46(3): 515-533. <https://doi.org/10.1016/j.cvsm.2015.12.008> PMid:27068445
3. Samii, V.F., Biller, D.S., Koblik, P.D. (1998). Normal cross-sectional anatomy of the feline thorax and abdomen: comparison of computed tomography and cadaver anatomy. *Vet Radiol Ultrasound.* 39(6): 504-511. <https://doi.org/10.1111/j.1740-8261.1998.tb01640.x> PMid:9845186
4. Pendovski, L., Ilieski, V., Ursic, M., Petkov, V., Popovska-Percinic, F., Travnikar, B., Fazarinc, G. (2011). Anatomical correlation between dog transversal S10 plastinated thin sections and computer tomography (CT) images. *Proceedings of the Days of Veterinary Medicine* (pp. 124-125), Ohrid, R. Macedonia
5. Bozinovski, D., Popovska-Percinic, F., Petkov, V., Adamov, N., Nikolovski, M., Ilieski, V., Pendovski, L. (2018). Tools for interpretation of computer tomography (CT) split images at dog: study with S10 thin plastinated specimens (p. 200), Ohrid, R. Macedonia
6. Latorre, R., Arencibla, A., Gil, F., Rivero, M., Ramirez, G., Vaquezauton, J.M., Henry, R.W. (2003). P-40 and S10 plastinated slices: an aid to interpreting MR images of the equine tarsus. *J Int Soc Plast.* 18, 14-22.
7. Jones, D.G. (2002). Re-inventing anatomy: the impact of plastination on how we see the human body. *15(6):* 436-440. <https://doi.org/10.1002/ca.10040> PMid:12373732
8. Fasel, J.H.D. (1988). Use of plastinated specimens in surgical education and clinical practice. *1(3):* 197-203. <https://doi.org/10.1002/ca.980010306>

9. Pendovski, L., Ursic, J., Brankovic, V., Ilieski, V., Popovska-Percinic, F., Petkov, V., Travnikar, B., Fazarinc, G. (2013). Use of S10-thin plastinated slices for interpretation computer tomography (CT) scans: applied study for dog anatomy. Proceedings of the 7th Meeting of the Young Generation of Veterinary Anatomists, July, 17-20 (pp. 31), Leipzig, Germany
10. Pendovski, L., Petkov, V., Popovska-Percinic, F., Ilieski, V. (2008). Silicone plastination procedure for production of thin, semitransparent tissue slices: a study using the pig kidneys. *J Int Soc Plast.* 23, 10-16.
11. Şora, M.C. (2016). The general protocol for the S10 technique. *Res Clin Med.* 1(1): 14-18.
12. Sora, M.C., Latorre, R., Baptista, C., López, A.O. (2019). Plastination-a scientific method for teaching and research. *Anat Histol Embryol.* 48(6): 526-531. <https://doi.org/10.1111/ahe.12493> PMID:31573113
13. Pauline, S., Rabi, R.S., Sridhar, G., Suganthi, R. (2015). Comparison of CT numbers of organs before and after plastination using standard S-10. *Clin Anat.* 28(4): 431-435. <https://doi.org/10.1002/ca.22514> PMID:25708008
14. Stefanie, O., Gernot, Sc. (2007). Computed tomography in small animals - basic principles and state of the art applications. *Vet J.* 173(2): 254-271. <https://doi.org/10.1016/j.tvjl.2005.12.014> PMID:16516508
15. Rodríguez, M.J., Latorre, R., López-Albors, O., Soler, M., Aguirre, C., Vazquez, J.M., Querol, M., Agut, A. (2008). Computed tomographic anatomy of the temporomandibular joint in the young horse. *Equine Vet J.* 40(6): 566-571. <https://doi.org/10.2746/042516408x322166>
16. Arredondo, J., López, A.O., Agut, A., Gil, F., Soler, M., Rodriguez, M.J., Latorre, R. (2008). Epoxy plastinated slices of the temporomandibular joint of the cat are used to assess high resolution computed tomography. *J Int Soc Plast.* 23, 61-62.
17. Sora, M.C., Brugger, P.C., Strobl, B. (2002). Shrinkage during E12 plastination. *J Int Soc Plast.* 17, 23-27.
18. Donoso, E.S., Sora, M.C., Probst, A., Budrass, K.D., Konig, H.E. (2009). Mesoscopic structures of the equine toe demonstrated by using thin slice plastination (E12). *Wiener Tierärztliche Monatsschrift.* 96(11/12): 286-291.